Case Studies in Engineering Failure Analysis 8 (2017) 11–20

Contents lists available at ScienceDirect

Case Studies in Engineering Failure Analysis

journal homepage: www.elsevier.com/locate/csefa

Assessment of circumferential cracks in hypereutectic Al-Si clutch housings

M. Haghshenas[a,*], J. Jamali[b]

[a] Department of Mechanical Engineering, University of North Dakota, Grand Forks, USA
[b] Department of Mechanical Engineering, American University of the Middle East, Kuwait

ARTICLE INFO

Article history:
Received 21 September 2016
Received in revised form 16 November 2016
Accepted 28 November 2016
Available online 10 December 2016

Keywords:
Al-Si
B390.0
Hypereutectic
Microstructure
Crack
Silicon

ABSTRACT

As in situ natural composites with silicon phase acting as the reinforcing phase, Al-Si alloys are among most commonly used aluminum alloys in automotive applications (*i.e.* engine component). Silicon contributes to the strength of Al-Si alloys through load transfer from the Al matrix to the hard (rigid) Si phase in the microstructure (load-carrying capacity). Casting parameters (*i.e.* solidification rate, elemental segregation, secondary dendrite spacing . . .) as well as the size and distribution of the microstructural constituents in Al-Si alloys (*i.e.* morphology of Si particles, intermetallic compounds, secondary dendrite spacing) contribute directly to the mechanical response and failure (or fracture) behavior of the alloy within the service. In hyper-eutectic Al-Si alloys (*i.e.* B390.0), distribution of coarse pre-eutectic Si particle mainly contribute to stress concentration, crack initiation and propagation during the actual service condition. In the present paper, the parameters contribution to the formation of the circumferential cracks in clutch housings made of die cast hyper-eutectics B390.0 Al-Si alloys are assessed through optical microscopy and scanning electron microscopy. Casting variable, cooling rate, their effect on the cracks as well some of the possible causes are also discussed in detail.

© 2016 Published by Elsevier Ltd. This is an open access article under the CC BY-NC-ND license (http://creativecommons.org/licenses/by-nc-nd/4.0/).

1. Introduction

A combination of unique properties including high strength-to-weight ratio, high wear resistance, low thermal expansion, good machinability, good castability, and good vibration dampening is required in the transmission clutch housings to meet the functional requirements as expected in the new generation of vehicles. Al-Si alloys and in particular hypereutectic aluminum-silicon alloys are among top promising alternative materials for improving the tribological characteristics of connecting rods, clutch housings, brake drum and cylinder blocks [1–5]. Silicon is added to aluminum to increase stiffness, improve wear resistance and to maintain melt fluidity during casting. The microstructures of the hypereutectic Al-Si alloys could be considered as metal-matrix composites (MMC) reinforced by hard particles. In hypereutectic Al-Si alloys, a higher extent of Si increases the overall hardness of the alloy and therefore makes it more resistive to wear [6]. The Si content in the cast Al-Si alloys varies between 5 to 23 wt% depending on the composition of the alloys including hypo-eutectic, hyper-eutectic or eutectic according to the equilibrium binary diagram (Fig. 1). Properties of specific alloys depend upon the chemical composition (*i.e.* volume fraction of aluminum solid solution and silicon phase) of

* Corresponding author.
E-mail address: meysam.haghshenas@engr.und.edu (M. Haghshenas).

http://dx.doi.org/10.1016/j.csefa.2016.11.003
2213-2902/© 2016 Published by Elsevier Ltd. This is an open access article under the CC BY-NC-ND license (http://creativecommons.org/licenses/by-nc-nd/4.0/).

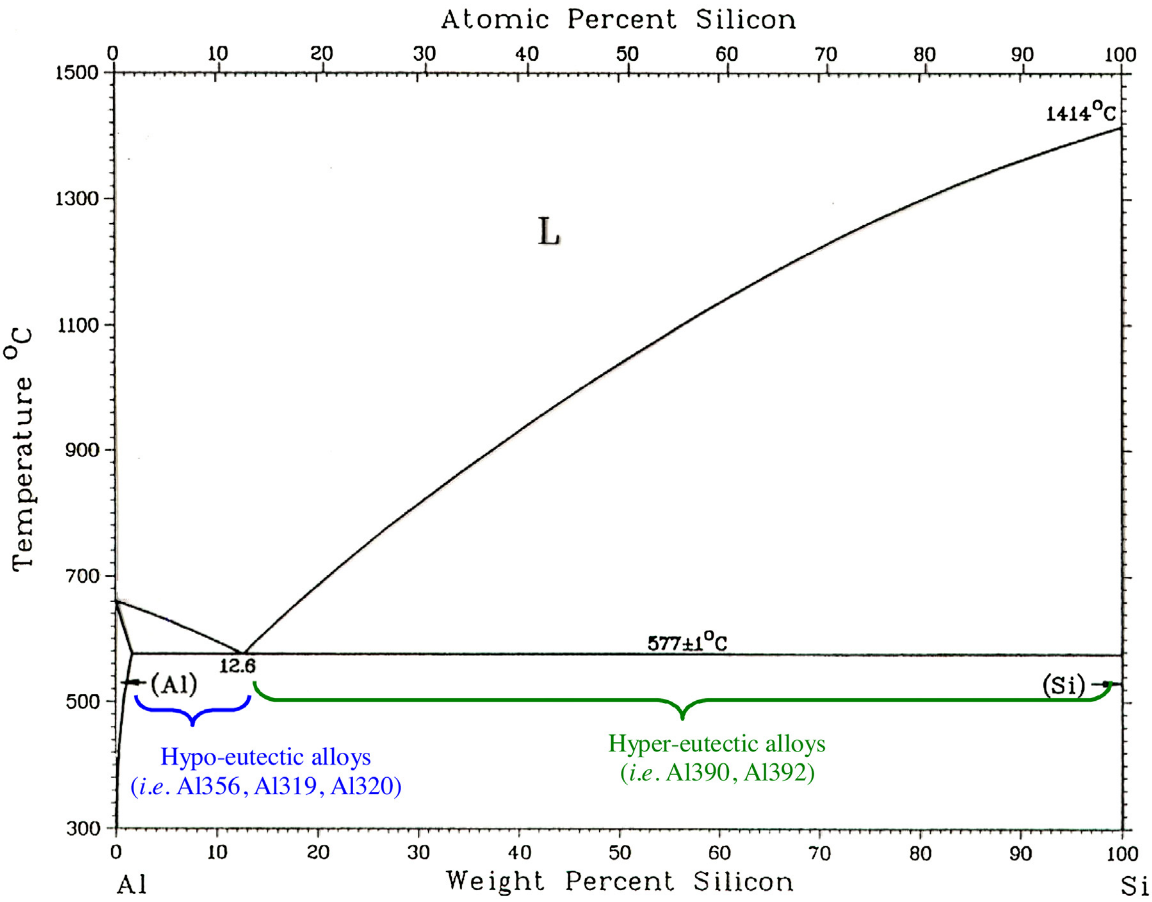

Fig. 1. Al-Si phase diagram showing hypo- and hyper-eutectic alloys.

the alloy as well as other parameters that act during solidification stage including cooling rate and liquid-solid temperature gradient [7,8].

Among Al-Si alloys, hyper-eutectic family (>12.6% Si) has been used in applications where high wear and strength resistance as well as low thermal expansion are needed [9,10]. The more Si an Al-Si alloy contains (*i.e.* high volume fraction of Si embedded in the aluminum matrix), the lower its thermal expansion coefficient will be; this characteristic and excellent wear resistance of hyper-eutectic Al-Si has made this family of Al-Si alloys as number one choice for vehicle engine applications, *i.e.* cylinder head, clutch housing and, blocks. Beside this, it is reported that high cycle fatigue strength of hypereutectic Al-Si alloys is 50% higher than hypoeutectic Al-Si alloys [11].

B390.0 is a hypereutectic Al-Si alloy which is over saturated with silicon (16–18% Si). During the formation of the alloy, silicon particles dissolve in the molten aluminum, while temperature rises, and become inseparable. However, below the eutectic point (12.6 wt% Si), while temperature decreases, silicon will not dissolve but rather precipitate out in crystalline form. Commercial grade hypereutectic Al-Si alloys range from 12.6 wt% to 20 wt% or more in silicon concentration. Primary crystalline Si particles enhance the hardness of the alloy and provide the required surface characteristic. Both volume and uniform distribution of primary Si particles play significant roles in wear resistance of hypereutectic Al-Si alloys for engine components [12]. Beyond 20% silicon concentration the alloys hardness reaches a level where it can no longer be machined using traditional machinery. Therefore in terms of minimizing casting costs for producing cylinder blocks, it is important that the material is machinable using standard tooling.

When a hypereutectic Al-Si alloy is chosen as the clutch housing material, the optimum micro structure for the casting is to have uniformly distributed primary silicon crystals in a eutectic Al-Si matrix. The uniformly distributed primary silicon particles are the key material characteristic for the clutch housing surface. Alloy 390 (ANSI/AA B390.0) was developed for automotive engine blocks; its resistance to wear is excellent but, its ductility is low. It is used for die cast valve bodies and sleeveless piston housings. Poor mechanical properties of B390.0 alloys in the actual service are attributed to the presence of coarse-faceted and brittle silicon particles (pro-eutectic silicon) and the resulting stress concentration in the microstructure [1,13].

Table 1
The nominal chemical composition of B390.0 alloy, wt%.

	Si	Fe	Cu	Mn	Mg	Ni	Zn	Ti	Al
B390.0	16–18	1.3	4.0–5.0	0.50	0.45–0.65	0.50	1.50	0.10	Bal.

It has been reported that the mechanical properties can be improved by changing the morphology and size of coarse lamellar silicon particles into small and finely distributed particles [14]. Beside chemical modifications and mechanical processing, silicon particle size and distribution can be controlled by changing the cooling rate during solidification; since Si particles are formed as the primary product of the eutectic reaction, increasing the cooling rate results in decreasing the Si particles size [15,16].

The present paper aims at describing a case study on assessment of circumferential cracks in a clutch housing found during the manufacturing stage. The material of the clutch housing part was a hypereutectic Al-Si alloy in as-cast condition. Microstructural examination of the failed part was done through optical and scanning electron microscopy. To this end,

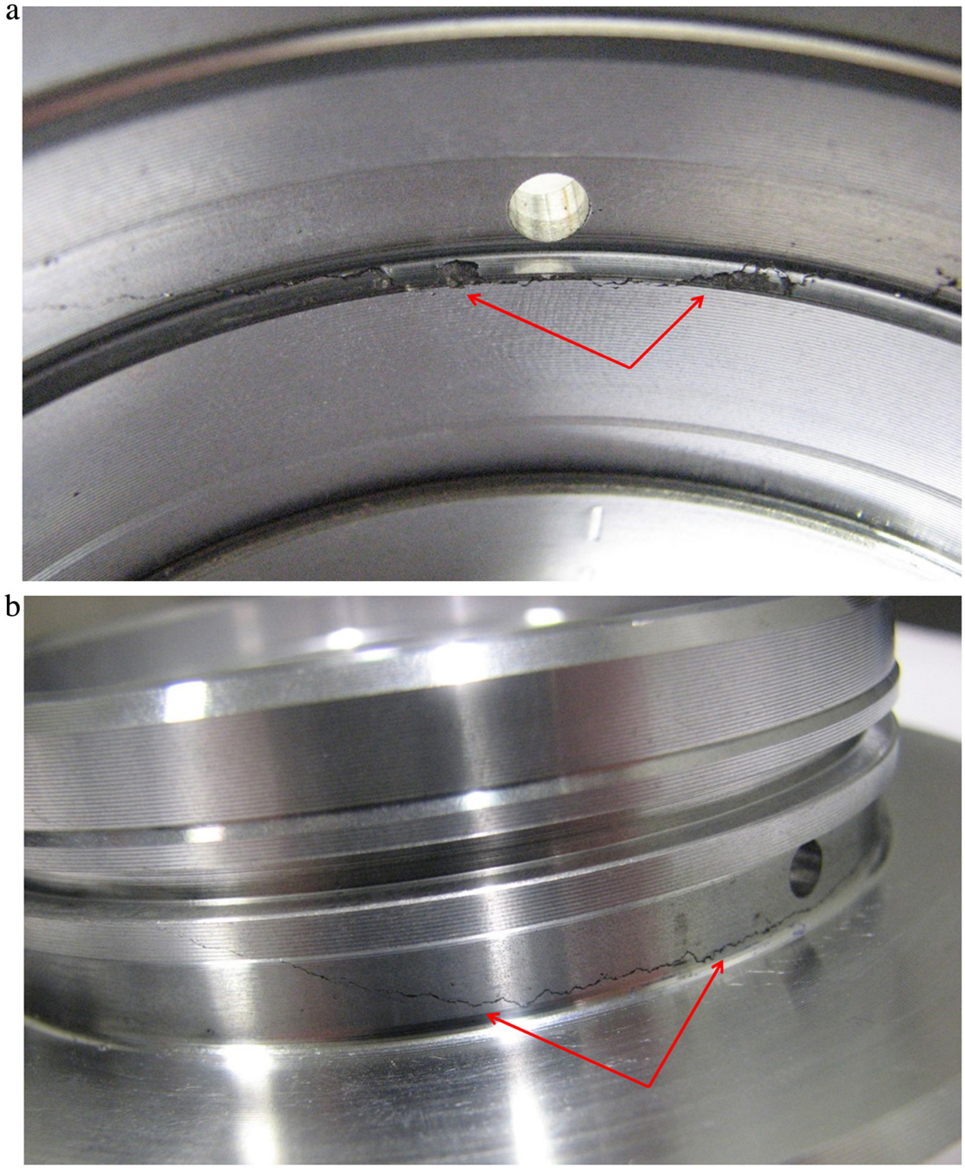

Fig. 2. The location of cracks on both sides; a) inside view of the crack, b) outside view of the crack. Red arrows show the crack path. Surface revealing crack is machined which made it possible to actually see the crack during the manufacturing process. (For interpretation of the references to colour in this figure legend, the reader is referred to the web version of this article.)

microstructural and mechanical assessments were performed through optical microscopy, scanning electron microscopy and hardness testing, respectively.

2. Experimental procedure

The starting cracked component is a die cast part of transmission out of B390.0 aluminum cast. Table 1 shows the nominal chemical composition of B390.0 which is a hyper-eutectic Al-Si alloy (Fig. 1).

Samples for optical microscopy were prepared from cracked specimens using a low-speed diamond saw. Using silica sandpapers, the transverse sections of the samples were coarse and fine polished using a 0.03–0.06 μ colloidal silica solution. After polishing, samples were etched with a 0.5 percent HF solution. Micrographs were taken using an optical microscope (OLYMPUS GX71) equipped with a digital camera and accompanying software on a PC. To assess the microstructure and identify different phases a scanning electron microscope (Quanta FEG 650) equipped with energy dispersive spectrometer (EDS) was employed. Vickers hardness testing (200 g) was used to record variation in the strength of the part around cracked region.

3. Results and discussion

3.1. Characteristics of the crack

The failed part contains a single, wide crack running through the entire circumference of the part (Fig. 2). No sign of deformation is visible in the plate indicating that the failure occurred in a brittle mode. Fig. 3 shows the SEM microstructure and EDS analysis of different spots of the failed part which consists of aluminum matrix with silicon particles as reinforcing phase. The primary Si is those light gray regions while white phases are different types of iron-rich intermetallic compounds

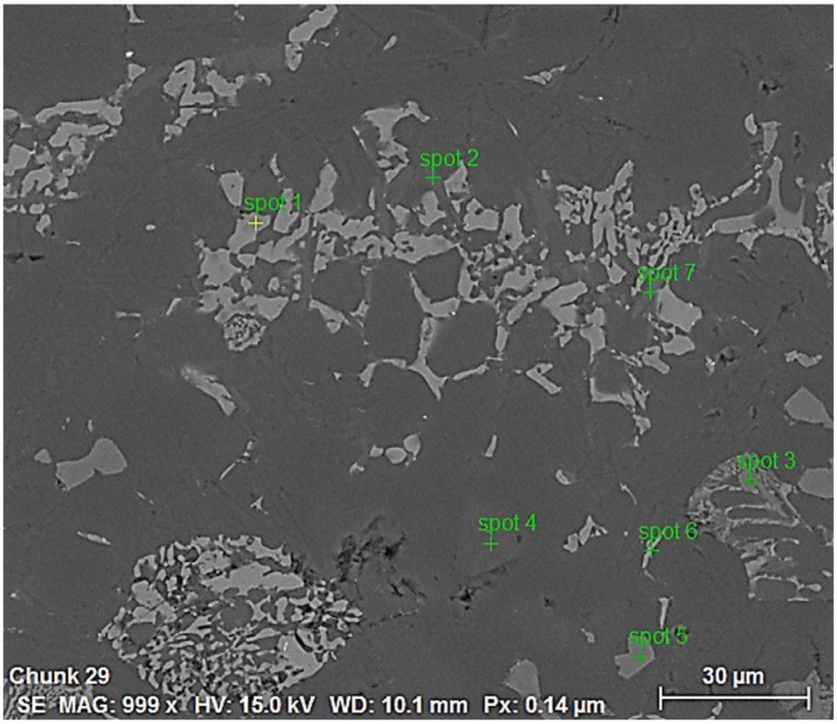

Spectrum	Mg	Al	Si	Cr	Mn	Fe	Ni	Cu
Spot 1		41.39	0.57			0.74		57.29
Spot 2	15.04	52.20	22.23		0.07	7.27	0.84	2.36
Spot 3	0.69	49.61	19.52		3.64	18.71		7.83
Spot 4			100					
Spot 5		59.15	8.80	2.10	6.26	20.66		3.02
Spot 6		59.98						40.02
Spot 7	23.49	26.50	21.38					28.64

Fig. 3. SEM image of the cracked Al-Si alloy including EDS analysis results of different spots in the structure, wt%.

(*i.e.* Al_5FeSi, $Al_{15}(Fe,Mn)_3Si_2$ [17,18]). Solubility of Fe in Al is very little, therefore, it forms various intermetallic compounds with Al and other elements.

Fig. 4 shows the optical micrograph of the failed (cracked) part near the fracture surface. As seen, the microstructure of the alloy around the crack are quite different; in the left side, grains, Si particles, and intermetallic compounds are quite coarse, however, in the right side fine structure is observed.

Fig. 5 shows the cracked region at higher magnification. From left to right the microstructure can be divided to (*i*) coarse-sized structure, (*ii*) crack, (*iii*) fine-grained structure, and (*iv*) medium-grained structure. Some gas porosities are also visible in Fig. 5. These defects act, at a minimum, to decrease the load bearing cross section and as crack nucleation sites.

It is reported that achieving homogeneous and uniform properties through casting process of the hypereutectic Al-Si alloys is quite challenging. Controlled casting of hypereutectic Al-Si alloys is very important because the tribological surface characteristics of hypereutectic Al-Si cylinder bores greatly depend upon even dispersion of Si particles [12,19].

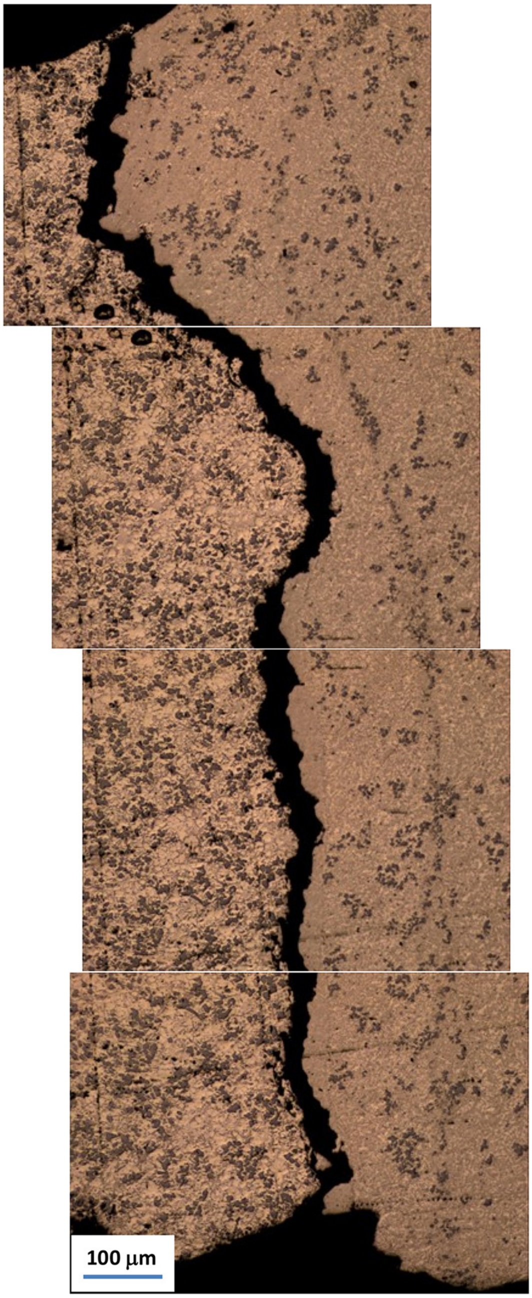

Fig. 4. Optical micrograph of the through-thickness crack showing the crack path and surrounding structures.

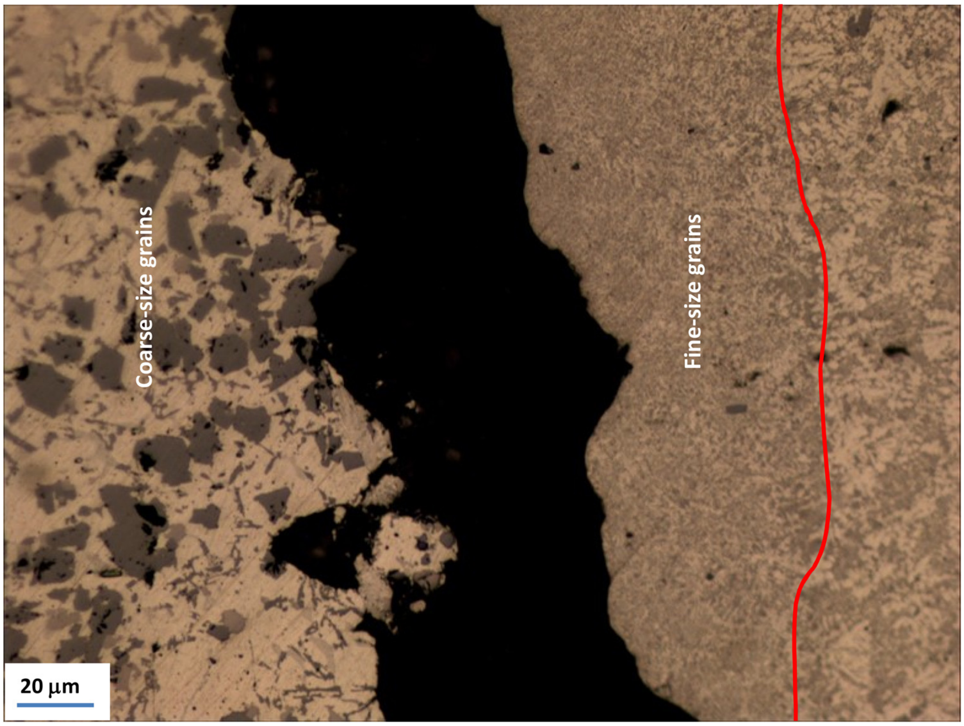

Fig. 5. Higher magnification of the crack and the surrounding structures including course, fine, and medium grain size. Red line is the border between fine and coarse grain sizes. (For interpretation of the references to colour in this figure legend, the reader is referred to the web version of this article.)

Different grain sizes observed in Figs. 4 and 5, can be attributed to different cooling (and solidification) rates happened inside the die during casting process. Finer grain area corresponds with the higher cooling rate which is typical for surface solidification of metal. As the solidification time is shorter, less time will be available for the diffusion of the hydrogen into the inter-dendritic regions resulting in lower volume fraction of pores near the surface. Also, increasing the solidification rate reduces the time during which solid state diffusion state may take place which results in a lower concentration of Si in solid solution. These effects result in refinement of grains and phases (*i.e.* Fe-Si intermetallic compounds), modification of acicular eutectic Si, and suppression of detrimental precipitates [20]. It is reported that increasing the cooling rate causes a change in the morphology and magnitude of Fe-rich intermetallic (*i.e.* Al_4FeSi_2, Al_5FeSi) compounds.

The left side of the crack includes large Fe-intermetallic compounds and coarse pro-eutectic Si phase revealing that the rate of cooling is quite slow. These coarse phases, formed at a slow cooling rate, are detrimental to the mechanical properties. However, on the right side with higher cooling rate, the solubility of Si in Al-matrix increases and density and distribution of pro-eutectic Si gradually decreases. Higher dissolution of Si content in Al-matrix results in the fragility of the alloy promoting the crack susceptibility.

3.2. Casting parameters

The rate of advance of the solidification interface in Al-Si alloys depends on two parameters [21]: (*i*) the balance between the rate of heat flow from the liquid to the solid through the interface and (*ii*) the latent heat of fusion released during solidification. Latent heat of fusion of Si (1411 J/g) is more than 3.5 times of aluminum (396 J/g) while its thermal conductivity is just 40% of aluminum thermal conductivity. This results in faster solidification rate in Al compared with Si. As seen cooling rate possesses a significant effect on the microstructure (*i.e.* grain size) and in particular characteristics of Si particles (*i.e.* size, morphology, distribution). Increasing cooling rate results in finer grains and intermetallic compounds size as well as smaller eutectic Si particles size [22]. Poor ductility was found in microstructures solidified at low cooling rates (>1 °C/s) that showed an overgrowth of primary Si in the Al matrix, as well as a large fraction of coarse acicular eutectic Si. On the other hand, rapid cooling may produce fragility in thin-section castings.

Beside a primary through crack, some secondary cracks in silicon particles and Fe-rich intermetallics are also visible along with the principal crack and are mostly confined along the silicon particles (Fig. 6a). These cracks are shown with a red arrow in Fig. 6a. Under applied external stresses during manufacturing (*i.e.* machining) or service, Al matrix experiences plastic deformation around Si platelets (and Fe-rich particles) resulting large stress mismatch and stress concentration which reduces the toughness and crack resistance of the component. Indeed, tips and terminals of these hard (and brittle) phases act as stress riser points upon which crack nucleates in the Al matrix and propagate through hard and stiff phases (Si and

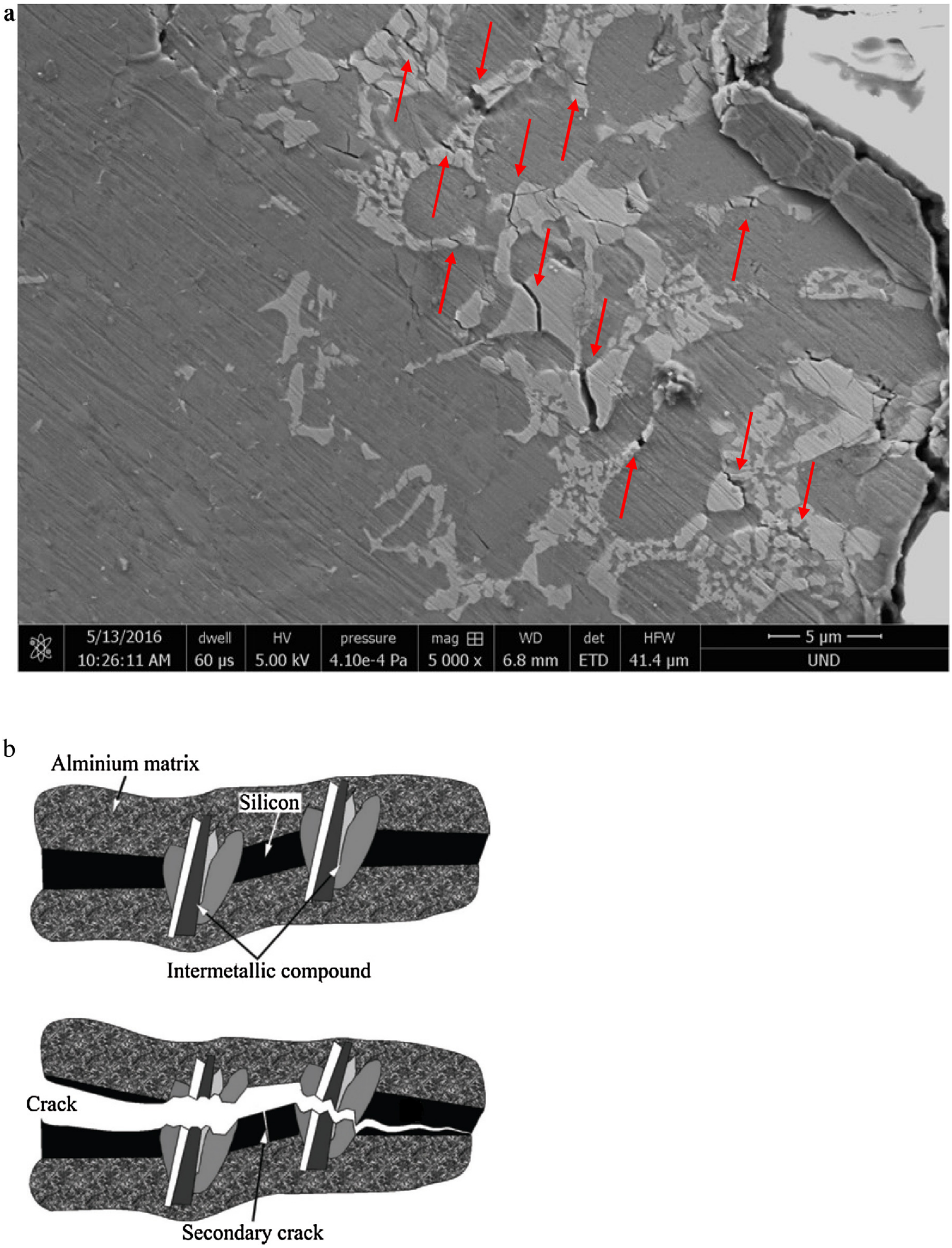

Fig. 6. a) cracked Si particles and Fe-rich phases along with the principal crack, b) Schematic illustration of the fracture mechanism including starting microstructure of Al-Si alloy and propagation stage of crack along Al–Si interfaces and breakup of blocking intermetallic particles [25].

Fe-rich) upon loading (Fig. 6b) [6,23]. It worth noting that the presence of these secondary cracks weakens matrix (de-bonding of the silicon/Fe-rich particles from the matrix and propagation (coalescence) of cracks through cleavage of these brittle phases) and thus more tight control of solidification rates is extremely important.

During actual service, cracks are initiated in the silicon particles or at the interface of Si particle and aluminum matrix, then the damage grows and micro-cracks are formed. These micro-cracks then link to each other and crack propagates (Fig. 7). In Al-Si alloys, crack initiation mainly occurs due to stress incompatibility and low bonding strength between ductile aluminum matrix and brittle Si particles. Due to de-bonding between Al and Si, micro-voids are formed at the Al/Si interface; then these micro-voids may interconnect to each other within actual service under applied stresses/strains and form the principal macro-crack [24]. Sometimes the fracture is dominated by the iron-rich intermetallics, and Si particles. In hyper-eutectic Al-Si alloys, the fracture seems of an intergranular failure mode where coarse pro-eutectic Si particles and Fe-rich intermetallic compounds are present. Iron possesses very low solubility in aluminum and this results in the formation of various Fe-rich phases (*i.e.* spots 2, 3, 5) which are hard and brittle. Therefore, these phases tend to have a relatively low bond strength to the matrix resulting in co-participation of these iron-rich intermetallics and the Si particles in the damage events. For engineering applications (where ductility and toughness are critical), the Fe-content of the alloys should be kept at a minimum level Fig. 7.

3.3. Mechanical properties

In general, the impact strength of Al-Si alloys is quite low which makes them a fragile alloy in impact applications. For instance, the impact energy of hypereutectic Al-Si alloys varies between 4 and 12 J/cm^2 [25,26]. The main reason for such small impact energy in hypereutectic Al-Si alloys is the presence of hard and brittle Si particles and intermetallic compounds embedded in a ductile (aluminum) matrix. These particles can act as stress concentration (and crack initiation) sites through which crack can propagate even upon applying small impacts. One way to improve crack resistance of these alloys is silicon spheroidization though chemical modifications, heat treatment and thermomechanical processing. By spheroidization, sharp tips and terminals of Si particles (and intermetallic compounds) are eliminated thus improving impact strength and other mechanical properties [17].

To measure the hardness variations in the cracked region Vickers hardness testing with 200 g f load was used. Fig. 8a shows the indentation prints around the cracked region and Fig. 8b shows the corresponding variation in hardness (hatched area corresponds to crack path). As seen, on the left side of the crack in which coarse particles are present, large variations in

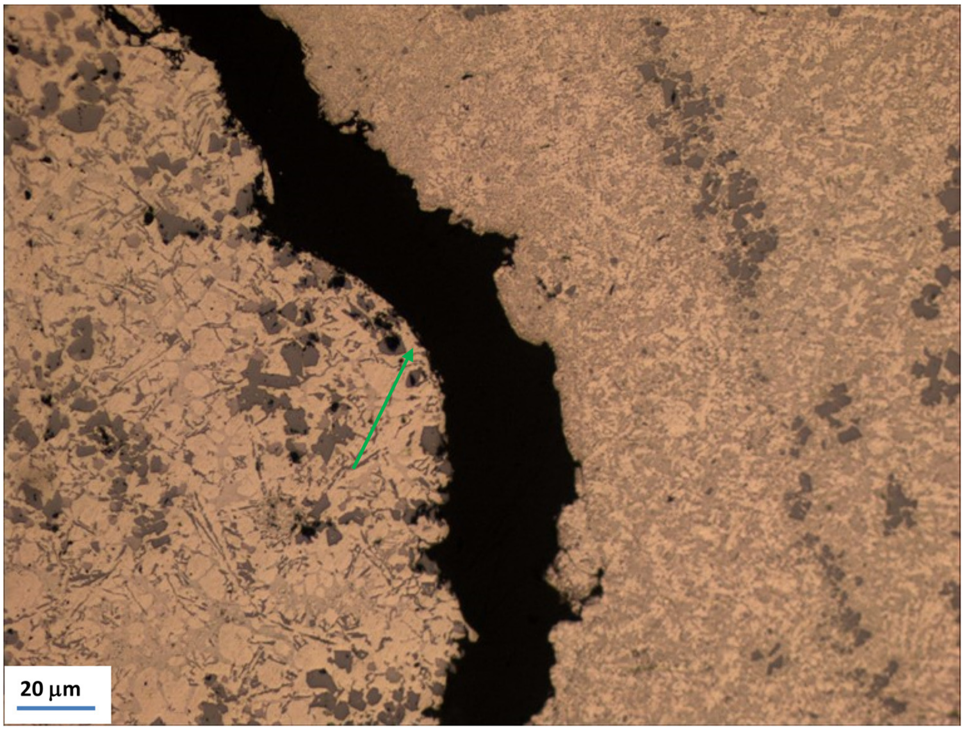

Fig. 7. The crack and the structure around it. On the left hand side the surface of the solidified melt is smooth (green arrow). This is an indication of absence of fusion. Crack formation usually results in a rough surface on opening. This is because of the way crack propagates. The smooth surface, in this case, can only come from molten metal and it will be representative of solidified surface of the melt. It is always smooth – surface tension of melt. (For interpretation of the references to colour in this figure legend, the reader is referred to the web version of this article.)

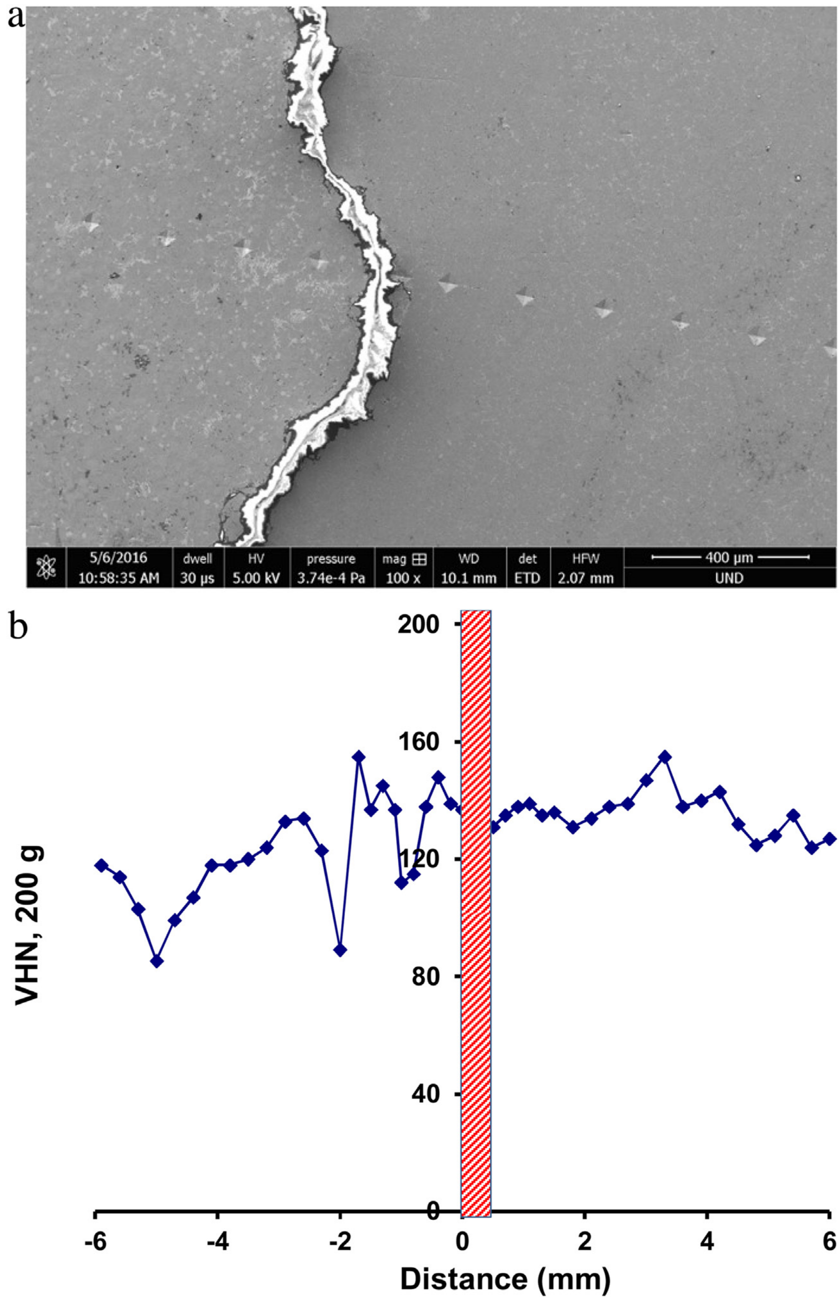

Fig. 8. a) Vickers indenter prints on the cracked face, b) corresponding variations in hardness (the distance is measured from the crack).

hardness points exist; however, less scatter in hardness points is seen on the right side of the principal crack path where particles are finer and more evenly distributed.

By doing point analysis through EDS different phases in the microstructure were individually analyzed. The corresponding compositions of the major elements are presented in Fig. 3. Dark colored phase in the microstructure corresponds to primary silicon particle while the composition of bright-colored phase is closely related to the Fe-rich intermetallic phase (*i.e.* Al_5FeSi).

4. Conclusions and remedial actions

The microstructure of the studied Al–Si alloy was mainly composed of primary and eutectic silicon particles along with iron-rich intermetallic compounds. During manufacturing and subsequent finishing (*i.e.* machining), the part showed a typically brittle fracture mode.

1. Differences in morphology between two sides of the crack are indicative of different solidification and, probably, cooling rates of two streams of metal in the cavity that met each other in the point where fracture observed.
2. Control of solidification rate is very important for preventing material failure under load. Solidification rate of metal is directly related to pouring temperature, and chemical composition of the alloy being used. Inaccurate controlling of these parameters may result in hot tearing phenomenon which is very probable in this alloy because of its large mushy (solid & liquid) zone as well as large thermal/mechanical stresses during the actual service.
3. Differenced in solidification rates are probably resulted from either non-uniform cooling of cavity, issues with overflow cavities, or cavity preheating.
4. Brittle silicon and iron-rich intermetallic phases act as easy crack paths, linking the particle fractures together and leading to an uncontrolled fracture of the material.

Acknowledgment

First author would like to acknowledge valuable comments by Dr. Walter Savich.

References

[1] Hekmat-Ardakan Alireza, Ajersch Frank. Acta Mater 2010;58:3422–8.
[2] Chen M, Alpas AT. Wear 2008;265:186.
[3] Ott RD, Blue CA, Santella ML, Blau PJ. Wear 2001;251:868.
[4] He Kezhun, Yu Fuxiao, Zhao Dazhi, Zuo Liang. J Alloys Compd 2012;539:74–81.
[5] Kapranos P, Kirkwood DH, Atkinson HV, Rheinlander JT, Bentzen JJ, Toft PT, J Mater Process Technol 2003;135:271–7.
[6] Ye Haizhi. J Mater Eng Perform 2003;12:288–97.
[7] ASM International. Chapter 1: introduction to aluminum-silicon casting alloys. Aluminum-Silicon Casting Alloys: Atlas of Microfractographs. .
[8] Nikanorov SP, Volkov MP, Gurin VN, Burenkov Yu A, Derkachenko LI, Kardashev BK, Mater Sci Eng A 2005;390:63–9.
[9] Maeng Y, Lee JH, Won CW, Cho SS, Chun BS. J Mater Process Technol 2000;105:196–203.
[10] Long S, Zhang Z, Flower HM. Acta Metall Mater 1994;42(4):1389.
[11] Valtierra-Gallardo S, Talamantes-Silva A, Rodrı′guez-Jasso, Gonaza′ lez-Villarreal JA. US Patent, 0031768 Al. Feb. 7.
[12] Javidani Mousa, Larouche Daniel. Int Mater Rev 2014;59:132–58.
[13] Wang Feng, Ma Yajun, Zhang Zhengye, Cui Xiaohao, Jin Yuansheng. Wear 2004;256:342.
[14] Mahmoud TS. Surf Coat Technol 2013;228:209–20.
[15] Matsuura K, Kudoh M, Kinoshita H, Takahashi H. Mater Chem Phys 2003;81:393–5.
[16] Ohmi T, Kudoh M, Ohsasa K, Itoh Y, Matsuura K, Ishii K. J Light Met 1994;44:91.
[17] Chandra K, Kain Vivekanand. J Fail Anal Prev 2015;15:679–85.
[18] Seifeddine S, Svensson IL. Metall Sci Technol 2009;27–1:11–20.
[19] Fuoco R, Moreira MF. AFS Trans 2009;117:225–40.
[20] Suarez Miguel Angel, Figueroa Ignacio Figueroa, Cruz Alejandro, Hernandez Alfredo, Chavez Jose Federico. Mater Res 2012;15(5):763–9.
[21] Requena G, Garcés G, Rodríguez M, Pirling T, Cloetens P. Adv Eng Mater 2009;11:1007–14.
[22] M.R. Zamani, MSc. Thesis. Department of Materials and Manufacturing, School of Engineering, Jönköping University. SE-551 11. Jönköping. Sweden.
[23] Onyia CW, Okorie BA, Neife SI, Obayi CS. World J Eng Technol 2013;1:9–16.
[24] Zhang Guo-hua, Zhang Jian-xin, Li Bing-chao, Cai Wei. Prog Nat Sci Mater Int 2011;21:380–5.
[25] Paray F, Kulunk B, Gruzleski JE. Int J Cast Met Res 2000;13:17–37.
[26] Ma A, Suzuki K, Saito N, Nishida Y, Takagi M, Shigematsu I, Mater Sci Eng A 2005;399:181–9.